Morphology and Physical Properties of Closed-Cell Microcellular Ethylene–Propylene–Diene Terpolymer (EPDM) Rubber Vulcanizates: Effect of Blowing Agent and Carbon Black Loading

K. C. GURIYA and D. K. TRIPATHY*

Rubber Technology Centre, IIT, Kharagpur 721302, India

SYNOPSIS

The morphology of the microcellular ethylene–propylene–diene terpolymer (EPDM) vulcanizes of both an unfilled and filled compound was studied from SEM photomicrographs. Carbon blacks adversely affect the average cell size, maximum cell size, and cell density. Enclosed gas pressure in a closed cell increases the relative modulus at higher strain. Tensile strength decreases more steeply than the expected value obeying the additive rule. At higher temperature, tensile strength, elongation at break, and modulus values decrease. The stress-relaxation behavior is independent of blowing agent loading, i.e., the density of closed-cell microcellular rubber. The elastic nature of the closed cell, i.e., the gas bubble in the microcellular rubber, reduces the hysteresis loss compared to solid rubber vulcanizates. Theoretically calculated flaw sizes are found to be about 3.4 times larger than the maximum cell sizes observed from SEM photomicrographs. It reveals that tear path deviates from the linear front and gives an effective larger depth of the flaws. © 1996 John Wiley & Sons, Inc.

INTRODUCTION

Industrial and commercial applications of microcellular rubbers demand strong, smooth skin and uniform cell structure. Close control of the foamed structure depends on the proper selection of blowing agents and curative to achieve the correct balance between gas generation and degree of cure. The cellular and microcellular ethylene–propylene–diene terpolymer (EPDM) has found increasing application in automobile sectors due to its good aging properties and high filler loading capacity. Systematic studies of the properties of cellular and microcellular rubber have not received much attention. In contrast to the thermoplastic foams, only a few articles on the expansion and curing behavior of the rubbers have appeared in the literature.[1-3] Previous studies on elastomeric foams[4-8] were primarily concerned with the development of compounding techniques for various elastomers and studies of their physical properties like tensile strength, compression deflection, water absorption, and ozone resistance. The morphology of elastomeric foam[9] and characterization of microcellular foam[10] have also been reported. Mechanical properties and modeling of cellular materials (polymers, ceramics, and metals) have been published by several authors.[11-13] Theoretical modeling of the elastomeric latex foam has been developed by some authors for both open- and closed-cell foam to predict the failure properties.[14-17] The mechanism of nucleation and bubble growth in elastomers,[18] thermoplastics,[19] thermoplastic elastomers,[20] and microcellular thermoplastics[21-23] using a blowing agent and a supersaturation method have been the subject of recent research. Recently, the physical properties of cellular and microcellular rubbers such as hysteresis, damping, cell size, and thermal insulation properties have been reported in the literature.[24-28]

In the present study, we emphasized the processing and compounding techniques to achieve closed-cell microcellular rubber with uniform cell-size dis-

* To whom correspondence should be addressed.

Journal of Applied Polymer Science, Vol. 62, 117-127 (1996)
 CCC 0021-8995/96/010117-11

tribution. We also studied the morphology and physical properties of the microcellular EPDM rubber with special reference to the variation of blowing agents and carbon black loadings.

EXPERIMENTAL

Materials

EPDM rubber (Kelton 520, ethylene content 55 mol %, diene content 4.5 mol % [DCPD], specific gravity 0.86, manufactured by DSM Chemicals, Holland) was used. HAF black (N330) was used as the filler, manufactured by Philips Carbon Black, India. The dicumyl peroxide (DCP) used was percidol 540C (40% DCP) manufactured by Chemoplast (I) Ltd. Dinitroso pentamethylene tetramine (DNPT), the blowing agent, was manufactured by High Polymer Labs, India.

Compounding and Sample Preparation

The rubber was compounded with the ingredients according to the formulations of the mixes (Table I). Compounding was done in a laboratory-size two-roll mill at room temperature according to ASTM D3182. Cure and blowing characteristics of the compounds were determined in a Monsanto rheometer, R-100. The vulcanizates were press-molded at 160°C to obtain a closed-cell microcellular sheet. As the press is closed, the compounds completely fill the mold, expelling the air and sealing the cavity. The typical compound flows readily in the molds, coalesces, and eliminates trapped air blisters. As the stock temperature increases, the cure starts and the decomposition of the blowing agent begins. Nitrogen is released and the cell starts to form. As the decomposition progresses, an exotherm develops and pressure builds up. These factors accelerate the curing rate. The press is opened before the cure has been completed. A very small closed cell is obtained after expansion. The precured sheet is postcured at 100°C for 1 h to complete the curing.

Test Procedures

The specific gravity of the samples was measured according to ASTM D 3574-77. The hardness of the microcellular sheets was measured using a Shore A durometer as per ASTM D 676-59T. Stress–strain properties like tensile strength, modulus, and elongation at break were measured on a computerized Zwick Universal Testing Machine according to ASTM D 3574-77. Cresent tear strength and trouser tear strength of microcellular rubber vulcanizates were also measured in the Zwick as per ASTM D 3574-77. Stress relaxation was measured according to ASTM D 3574-77. Measurement of hysteresis is also carried out in the same machine according to ASTM D 3574-77. All these tests were performed at room temperature (25 ± 2°C). At least five specimens per sample were tested for each property and the mean values are reported.

SEM Studies

SEM studies were carried out for understanding the cell structure using a Cam Scan Series 2 Model scanning electron microscope. Razor-cut surfaces from microcellular rubber sheets were used as samples for SEM studies. The samples were gold-coated before being studied.

RESULTS AND DISCUSSION

Rheometric Characteristics

The effect of blowing agents and carbon black (HAF) filler on the curing characteristics of the compounds is shown in the representative Monsanto rheograph (Figs. 1–3). The maximum rheometric torque decreases with increase in blowing agent loadings. The

Table I Formulations of Gum and Carbon Black Filled Vulcanizates

	Mix No.										
	G10	G12	G14	EB20	EB22	EB24	EB26	EB40	EB42	EB44	EB46
EPDM	100	100	100	100	100	100	100	100	100	100	100
Carbon black (HAF)	—	—	—	30	30	30	30	60	60	60	60
Paraffin oil	2	2	2	4.5	4.5	4.5	4.5	9	9	9	9
DNPT	0	2	4	0	2	4	6	0	2	4	6

Each mix contains ZnO, 2 phr; stearic acid, 2 phr; and dicumyl peroxide (40% DCP), 2 phr.

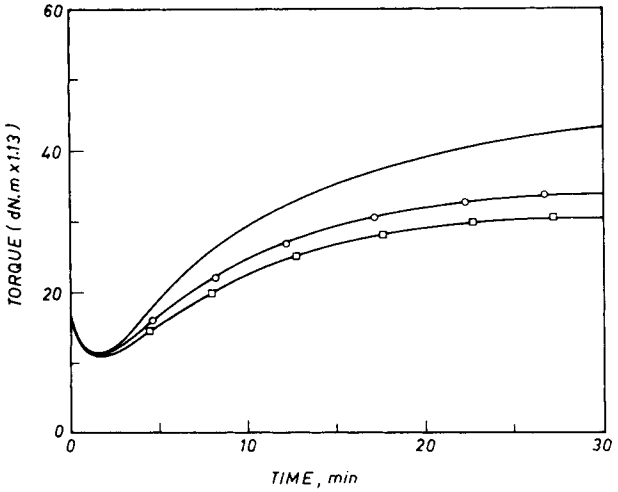

Figure 1 Representative rheographs of unfilled compounds: effect of blowing agent loading. (——) G10; (— ○ — G12; (— □ —) G14.

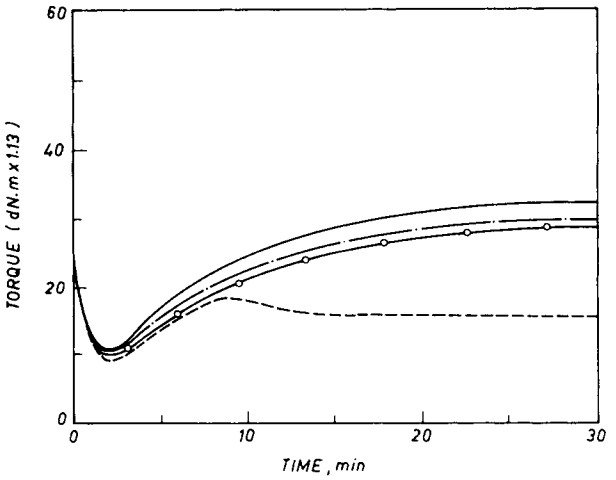

Figure 2 Representative rheographs of 30 phr carbon black filled compounds: effect of blowing agent loading. (——) EB20; (— · —) EB22; (— ○ —) EB24; (- -) EB24.

minimum rheometric torque also decreases slightly. During curing, the blowing agent starts decomposition. The decomposed gas either dissolves under high pressure or forms microbubbles in the rubber phase. These microbubbles reduce the shearing force. Hence, torque starts reducing at the onset of blowing agent decomposition and reaches an equilibrium stage. The curing is affected by the exothermic decomposition of the blowing agent. So, from this representative rheograph, actual cure characteristics cannot be obtained. But the resultant effect of curing and blowing can be obtained. At the higher blowing agent loadings (6 phr), 30 phr carbon black-loaded compounds show reversion of the torque and attain an equilibrium torque. This may happen when the blowing rate is higher than that of the curing rate. With increase in blowing agent loading, the equilibrium torque decreases due to the formation of more microbubbles.

Morphology of Razor-Cut Surfaces

SEM photomicrographs of razor-cut surfaces of various unfilled and filled microcellular rubber vulcanizates are shown in Figure 4. These photomicrographs are analyzed in terms of average cell size or diameter, maximum cell size, and cell density (number of cells per unit volume of the microcellular rubber). The number of cells increase as the blowing agent loadings increase. Average cell size decreases with increase in blowing agent loadings from 2 to 6 phr. Photomicrographs show that with filler loading the average cell size increases. The microbubbles formed by decomposition of the blowing agent diffuse and coalesce with each other due to decrease of the cure rate with increase in filler loading. Thus, with increased filler loading, average cell size as well as maximum cell size (l') increase (Table II). The number of cells of microcellular rubber vulcanizates at maximum expansion is calculated using the following relation[9]:

$$N = \frac{6}{\pi d^3}(\rho_s/\rho_f - 1)$$

where N is the number of cells per unit volume of rubber; d, the average cell diameter; and ρ_s and ρ_f, the density of the solid and microcellular EPDM

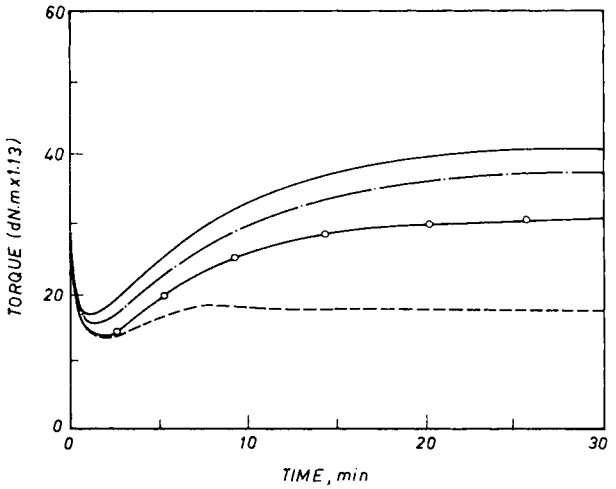

Figure 3 Representative rheographs of 60 phr carbon black filled compounds: effect of blowong agent loading. (——) EB40; (— · —) EB42; (— ○ —) EB44; (- -) EB44.

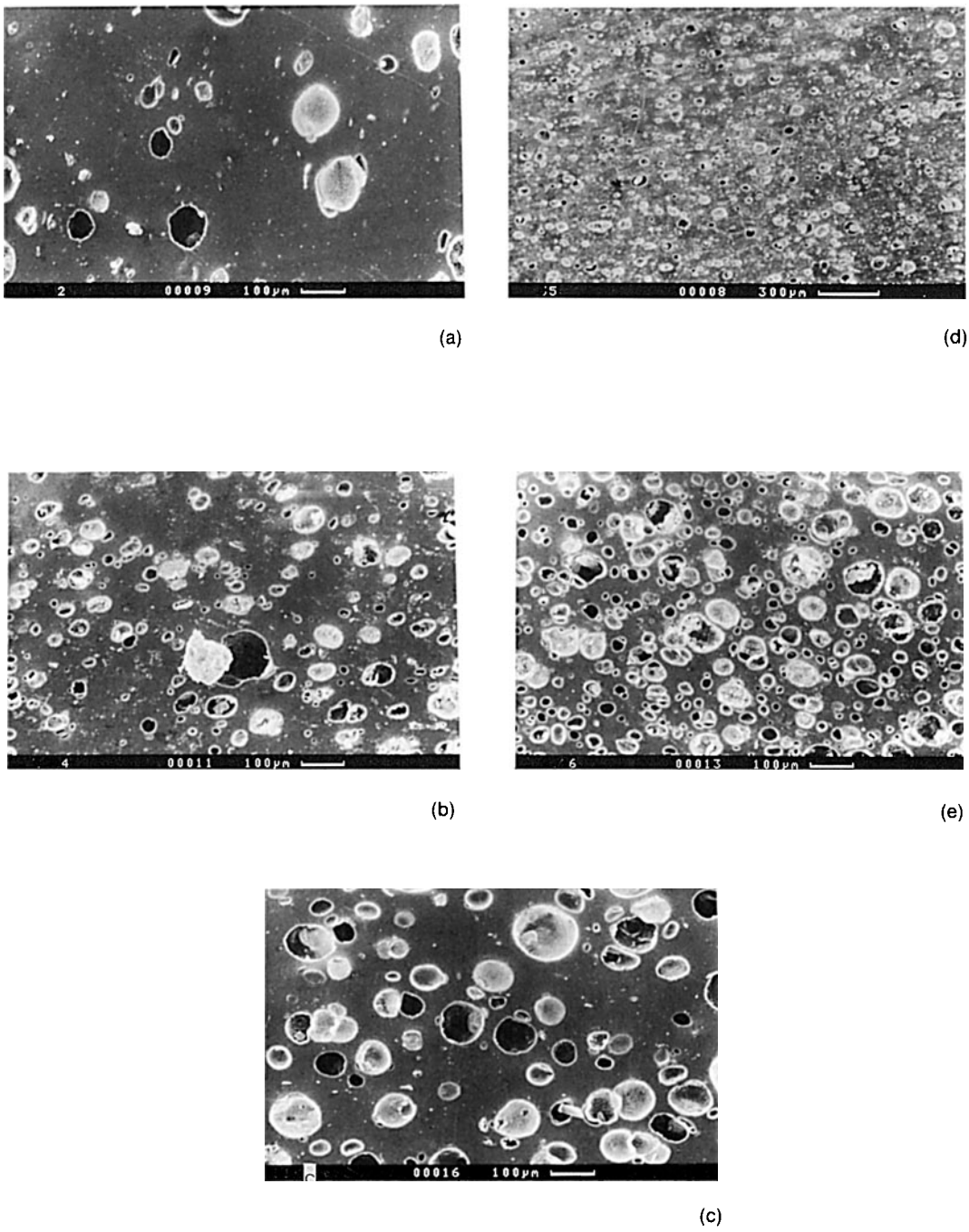

Figure 4 SEM photomicrographs of razor-cut microcellular rubber vulcanizates: (a) EB22; (b) EB24; (c) EB26; (d) G12; (e) EB44.

rubber vulcanizates, respectively. The number of cells per unit volume (cm^{-3}) are calculated and shown in Figure 5. The number of cells per unit volume increases with increase in blowing agent loading. The cell density decreases with increase in filler loading. The carbon black (HAF) filler, being basic in nature, does not act as a nucleating agent. This also reduces the acidity of filled compounds compared to the unfilled compounds which may result in a decrease in cell density.

Physical Properties

Physical properties like relative density, hardness, and tear strength are given in Table II. The relative density (ρ_f/ρ_s) decreases with increase in blowing

Table II Physical Properties of Unfilled and Carbon Black Filled Vulcanizates

Mix No.	Cell Size (μm)	Max^m Cell Size (μm)	Relative Density (ρ_f/ρ_s)	Hardness Shore A	Tear Strength (N/mm)
G10	—	—	1.00	38	13.29
G12	33	47	0.94	33	8.92
G14	32	40	0.88	32	9.92
EB20	—	—	1.00	45	42.54
EB22	53	100	0.845	40	72.90
EB24	40	75	0.824	35	65.20
EB26	26	81	0.718	34	54.49
EB40	—	—	1.00	55	40.81
EB42	100	125	0.905	48	90.88
EB44	60	143	0.77	40	65.70
EB46	37	93	0.613	27	43.42

agent loadings. The decrease in relative density is much more pronounced in filled compounds. With increase in filler loading, gas permeability decreases and, hence, there is less possibility of the loss of gas by diffusion. As a result, more gas remains in the rubber matrix. Thus, in filled compounds, the decrease in relative density is more for the same blowing agent loading. The hardness of the closed-cell microcellular rubber decreases with increase in blowing agent loadings. As the enclosed gas in the closed cell has little elastic property, hardness decreases with decrease in relative density.

Tear strengths of the closed-cell carbon black-filled microcellular rubbers are given in Table II. It is seen that tear strength increases compared to solid vulcanizates with incorporation of the blowing agent in carbon black filled vulcanizates. Also, tear strength is found to decrease with increase in the blowing agent loading. Exothermic decomposition of the blowing agent may cause excess crosslinking and, hence, tear strength increases. With increase in the blowing agent loading, the maximum cell size increases and, hence, the tear strength decreases.

Stress–strain plots of unfilled and carbon black loaded closed-cell microcellular rubber are illus-

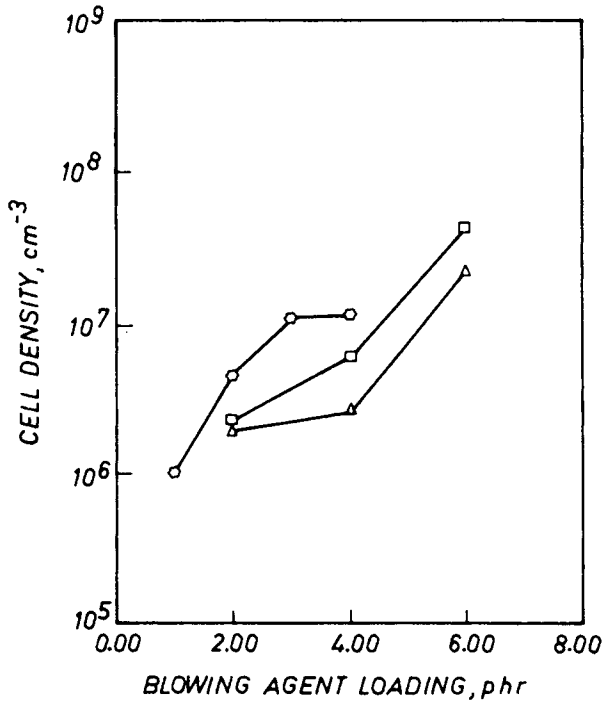

Figure 5 Effect of blowing agent loading on cell density of closed-cell microcellular rubber vulcanizates: (○) gum; (□) 30 phr black; (△) 60 phr black.

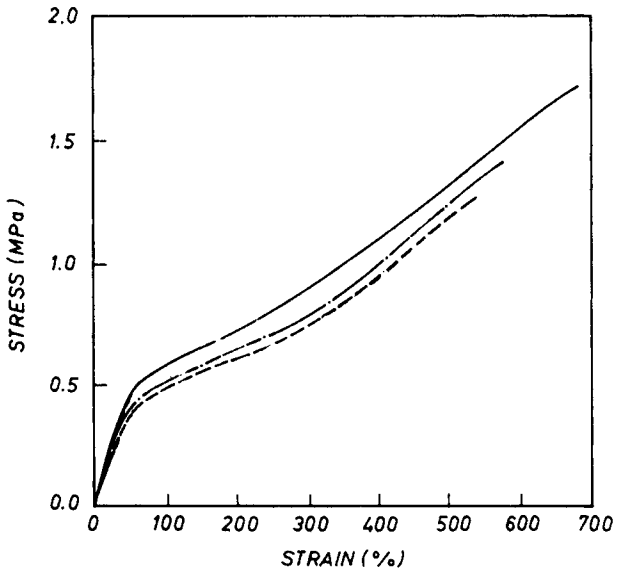

Figure 6 Stress–strain curves of closed-cell microcellular gum vulcanizates: (——) G10; (— · —) G12; (- -) G14.

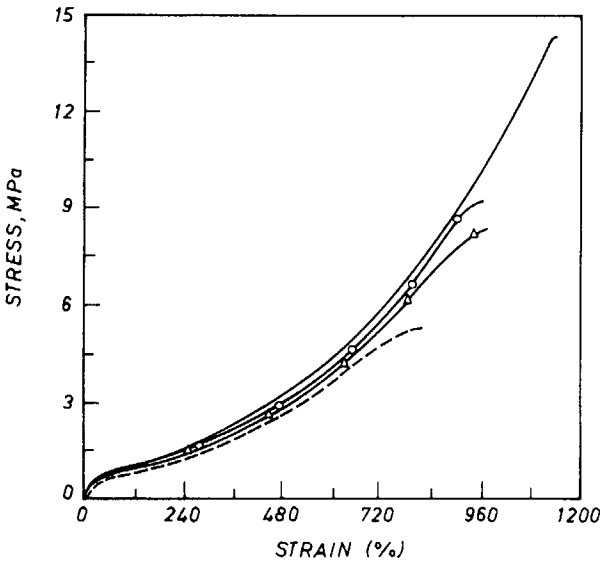

Figure 7 Stress–strain curves of 30 phr carbon black filled closed-cell microcellular rubber vulcanizates: (——) EB20; (— O —) EB22; (— △ —) EB24; (- -) EB24.

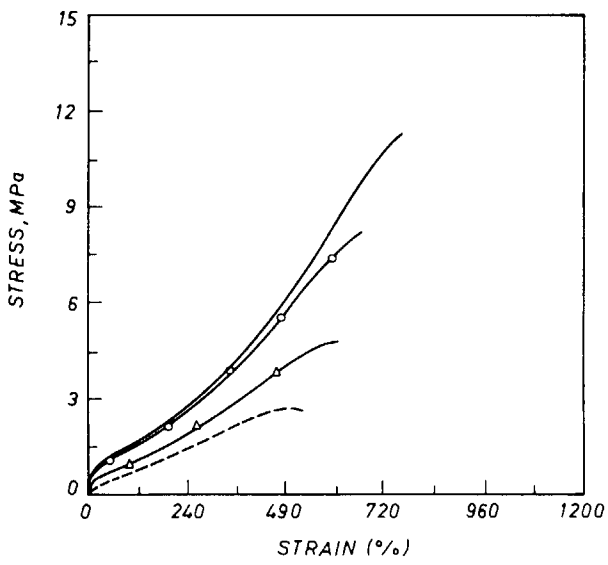

Figure 8 Stress–strain curves of 60 phr carbon black filled closed-cell microcellular rubber vulcanizates: (——) EB40; (— O —) EB42; (— △ —) EB44; (- -) EB44.

trated in Figures 6–8. Tensile strength, elongation at break, and modulus values of microcellular rubbers are tabulated in Table III. Tensile strength, elongation at break, and modulus values are decreased with increase in blowing agent loading. For filled samples, tensile strength and modulus increases for 30 phr filler loading, and with higher filler loading, tensile strength decreases but modulus increases. Tensile strength increases with strain in three distinct steps (Fig. 6). At small strain, closed-cell microcellular rubber shows the linear elastic modulus. This is caused by the cell edge bending, face stretching, and enclosed gas pressure.[14] Nonlinear elastic behavior of closed-cell microcellular rubber is observed at higher strain. The enclosed gas within the cells is compressed as the cell is stretched. Thus, membrane stresses appear in the cell faces and the stress–strain curve shows an increasing trend with strain. The axial stretching of cell walls is also responsible for increase in stress. At sufficiently large extension, the cell walls become stretched along the tensile axis and further extension will cause the elongation of the cell walls themselves. This will result in a steep rise of the stress–strain. Stress–strain plots of unfilled and carbon black-loaded closed-cell microcellular rubber at 70°C are illustrated in Figures 9 and 10. Tensile strength, elongation at break, and modulus values of micro-

Table III Physical Properties of Unfilled and Carbon Black Filled Microcellular Rubber Vulcanizates (Room Temperature)

Mix No.	Tensile Strength (MPa)	Elongation at (%)	Modulus 100%	Modulus 200%	Modulus 300%
G10	1.72	674	0.58	0.74	0.90
G12	1.42	570	0.51	0.64	0.77
G14	1.25	526	0.48	0.61	0.75
EB20	14.50	1150	0.90	1.24	1.80
EB22	8.80	988	0.82	1.20	1.68
EB24	8.30	960	0.74	1.08	1.63
EB26	5.40	810	0.63	0.96	1.47
EB40	10.50	750	1.32	2.19	3.40
EB42	8.20	678	1.28	2.12	3.25
EB44	4.7	560	0.96	1.60	2.45
EB46	2.8	500	0.69	1.25	1.85

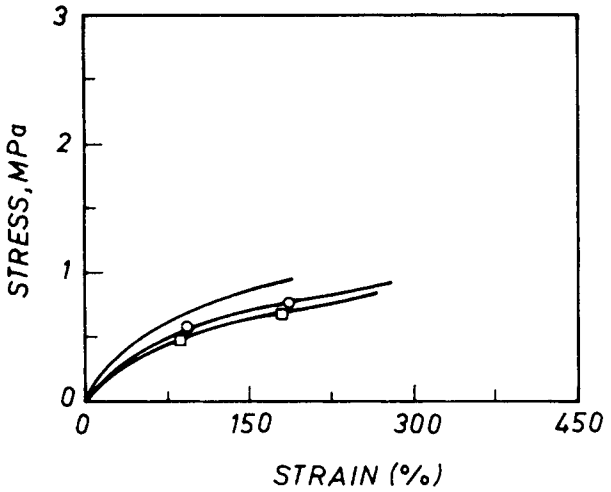

Figure 9 Stress–strain curves of closed-cell microcellular gum vulcanizates at 70°C: (——) G10; (— ○ —) G12; (— □ —) G14.

cellular rubbers at 70°C are also shown in Table IV. Tensile properties are found to decrease at higher temperature. This is due to the degradation and softening of the material.

In Figure 11, the relative modulus (σ_f/σ_s) and relative tensile strength (E_f/E_s) of 30 phr carbon black-loaded closed-cell microcellular rubber are plotted against relative density (ρ_f/ρ_s). The relative modulus, 100, 200, and 300%, and relative tensile strength decrease linearly with decrease in relative density. There is a sharper decrease in the relative tensile strength than in the relative modulus. Maximum cell size, i.e., flaws, affect the tensile strength but not the modulus. Thus, relative tensile strength behaves differently than does the modulus. The 300% relative modulus shows a higher value than 100% and 200% relative modulus. If the modulus depends only on the relative density, then it will follow the line joining (0, 0) and (1, 1) points according to the additive rule. So, this increase in relative modulus may be due to the increase in enclosed gas pressure within the cells.

The stress-relaxation behavior for closed-cell microcellular rubber is obtained by stretching the samples at a constant strain level of 100%. Figures 12 and 13 show the decay of stress with time for closed-cell microcellular rubber. The nature of the decay is almost similar for the closed-cell microcellular rubber. The rate of decay is more or less equal in solid and closed-cell microcellular rubber. It exhibits that the relaxation behavior is independent of blowing agent loading, i.e., the density of closed-cell microcellular rubber.

The hysteresis loss of unfilled and 30 phr carbon black-loaded closed-cell microcellular rubber at 100% elongation is shown in Figures 14 and 15. The hysteresis loss values are also given in Table V. The result exhibits that with increase in blowing agent loading the hysteresis loss decreases for all cycles of measurement. The incorporation of carbon black filler causes an increase in hysteresis loss. Solid vulcanizates (both unfilled and filled) exhibit higher hysteresis loss than that of the closed-cell microcellular vulcanizates. This low hysteresis loss of closed-cell microcellular vulcanizates can be attributed to the low-energy absorption characteristics of closed cells. The closed cell in the rubber matrix can act as elastic bodies and is incapable of dissipating energy. For the same reason, with increase in blowing agent loading, hysteresis loss decreases.

Fracture Nuclei in Tensile Failure

If the material breaks in simple extension by characteristic tearing from a small nick in one edge, the energy stored in the specimen at break, i.e., the work required to break, is simply related to the catastrophic tearing energy. The tearing energy of the foam, T_f, can be expressed as[14]

$$T_f = 2KE_f l \tag{1}$$

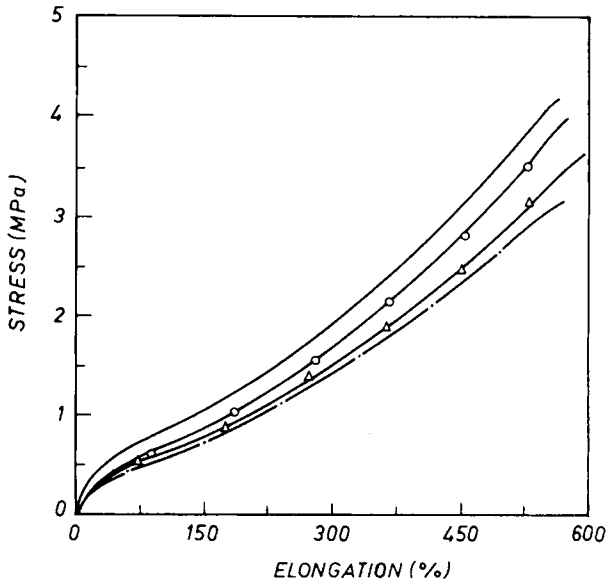

Figure 10 Stress–strain curves of 30 phr carbon black filled closed-cell microcellular rubber vulcanizates at 70°C: (——) EB20; (— ○ —) EB22; (— △ —) EB24; (- · -) EB24.

Table IV Physical Properties of Unfilled and Carbon Black Filled Microcellular Rubber Vulcanizates (at 70°C)

Mix No.	Tensile Strength (MPa)	Elongation at (%)	Modulus 100%	Modulus 200%	Modulus 300%
G10	0.98	188	0.73	—	—
G12	0.93	281	0.58	0.77	—
G14	0.88	263	0.55	0.75	—
EB20	4.14	544	0.84	1.35	2.03
EB22	3.92	564	0.66	1.10	1.72
EB24	3.64	588	0.62	0.98	1.52
EB26	3.17	575	0.54	0.92	1.42
EB40	3.88	350	1.22	2.01	3.14
EB42	3.65	378	1.08	1.89	3.03
EB44	2.47	326	0.81	1.38	1.98
EB46	1.58	295	0.48	0.98	1.52

where K is a numerical constant having a value of about 2,[14] l is the depth of the flaw, and E_f is the strain energy density in the bulk of the test piece for the foam. According to the tearing energy criterion developed by Rivlin and Thomas,[29] it can be assumed that tensile rupture occurs by catastrophic tearing of the flaw and is described by eq. (1). In the present work, the flaw depth (l) of the microcellular rubber vulcanizates were calculated from eq. (1) using the measured tear energy and strain energy density of the microcellular rubber vulcanizates. The tear energy was calculated from the tear strength using the trouser specimen (ASTM D-3574).[24] The following equation was used for the calculation of tear strength:

$$T_f = 2 \times \frac{F}{t} \tag{2}$$

$$T_f = 2 \times T'_f$$

where T'_f is the trouser tear strength and T_f is the tear energy. Strain energy density can be calculated from the tensile strength and the elongation at break of the dumbbell-shaped specimen. The results are summarized in Table VI. The maximum cell size or diameter (l') of the microcellular rubber vulcanizates were also measured from SEM photomicrographs of razor-cut closed-cell microcellular samples and the values are tabulated in Table VI. It is clear that the theoretical values[14] of the flaws depth (l) are larger

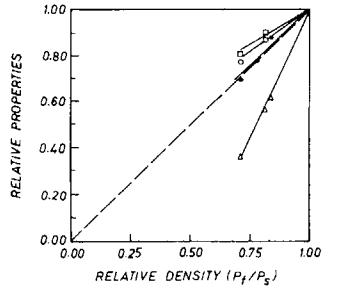

Figure 11 Effect of relative density (ρ_f/ρ_s) on relative properties of 30 phr carbon black filled microcellular rubber vulcanizates. (△) Relative tensile strength; (●) relative 100% modulus; (○) relative 200% modulus; (□) relative 300% modulus.

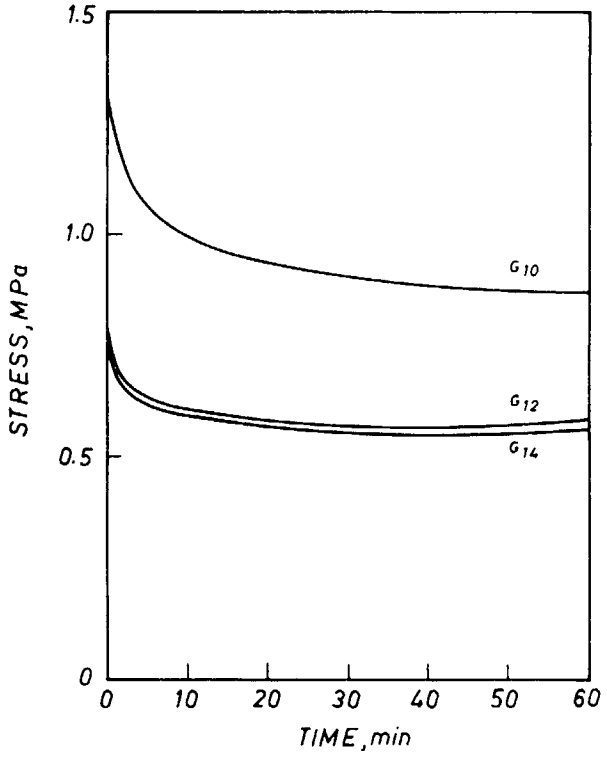

Figure 12 Stress-relaxation behavior of closed-cell microcellular gum vulcanizates.

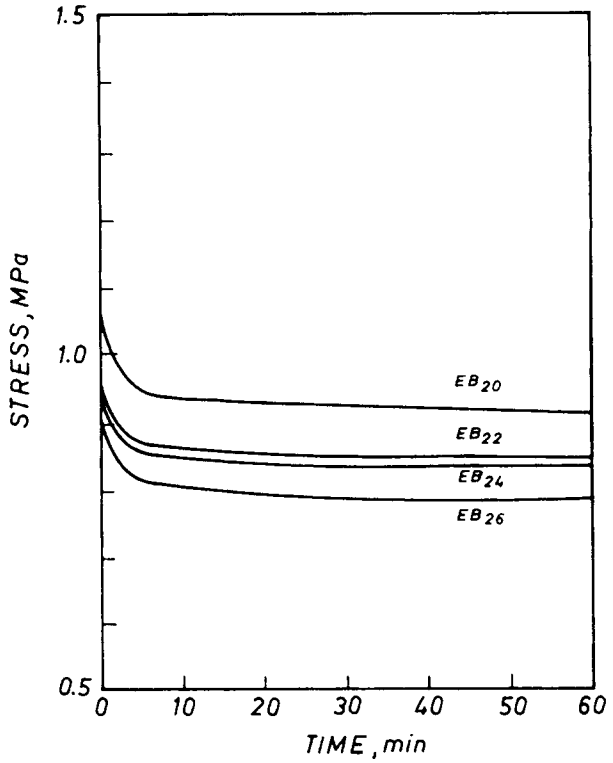

Figure 13 Stress-relaxation behavior of 30 phr carbon black filled closed-cell microcellular rubber vulcanizates.

than the corresponding maximum cell size. The mean values of the ratio of the theoretical depth of flaws and maximum cell size is about 3.4. The closed cells are randomly arranged in the microcellular rubber vulcanizates. Imperfections in the microcellular rubber will lead to local deviation of the tear from the linear front and, hence, give rise to a larger effective depth of the flaws.

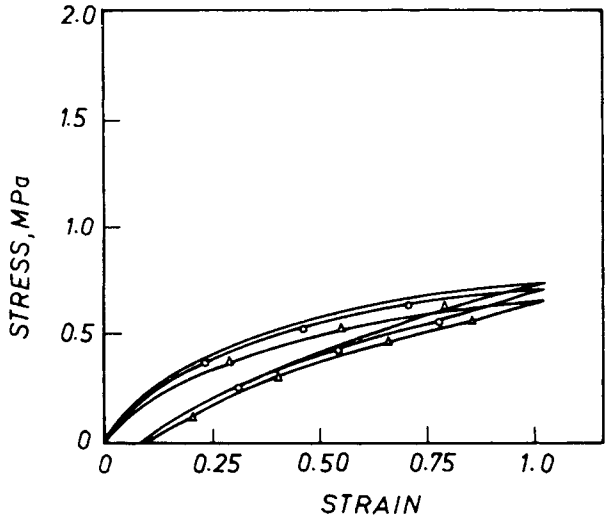

Figure 14 Hysteresis curves of closed-cell microcellular gum vulcanizates (first cycle): (——) G10; (— O —) G12; (— △ —) G14.

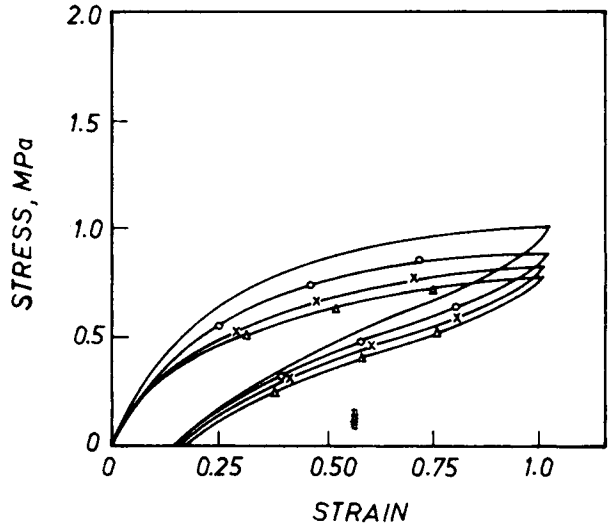

Figure 15 Hysteresis curves of 30 phr carbon black filled closed-cell microcellular rubber vulcanizates (first cycle): (——) EB20; (— O —) EB22; (— × —) EB24; (— △ —) EB24.

CONCLUSIONS

1. In the case of the microcellular EPDM rubber vulcanizates, the rheometric torque (maximum) decreases with increase in blowing agent concentration.

Table V Results of Hysteresis Studies of Unfilled and Carbon Black Filled Microcellular EPDM Rubber Vulcanizates

	Hysteresis Loss in J/m² at 100% Elongation		
Mix No.	1st Cycle	2nd Cycle	3rd Cycle
G10	0.00475	0.00264	0.00236
G12	0.00366	0.00215	0.00195
G14	0.00335	0.00192	0.00180
EB20	0.01598	0.00879	0.00739
EB22	0.01170	0.00780	0.00695
EB24	0.01136	0.00702	0.00672
EB26	0.00932	0.00602	0.00551
EB40	0.03075	0.01260	0.01111
EB42	0.02623	0.01198	0.00830
EB44	0.01880	0.00904	0.00813
EB46	0.01382	0.00682	0.00618

Table VI Tear Energy and Calculated Flaw Size of Carbon Black Filled Microcellular Rubber Vulcanizates

Mix No.	Trouser Tear Resistence (N/mm)	Tear Energy (T_f) (kJ/m^2)	Strain Energy Density (kJ/m^3)	Calculated Cell Size (l) (μm)	Max^m Cell Size (l') (μm)
G12	1.74	3.48	4047	215	47
G14	1.19	2.38	3287	181	40
EB22	13.73	27.46	43,427	157	100
EB24	12.05	24.10	38,400	156	75
EB26	10.88	21.76	21,870	248	81
EB42	22.77	45.54	27,798	409	125
EB44	18.44	36.88	14,880	619	143
EB46	11.24	22.48	7594	740	193

2. Average and maximum cell size increase with incorporation of carbon black filler. This effect is due to the alkaline surface of carbon black.
3. Cell density decreases with incorporation of carbon black filler. But with increase in blowing agent loading, cell density increases.
4. The relative density decreases with increase in blowing agent loading. This decrease is more pronounced in the case of carbon black filled compounds.
5. Incorporation of the blowing agent increases the tear strength with low blowing agent concentration, which, however, decreases with further increase in the blowing agent.
6. Tensile strength decreases with increase in blowing agent concentration in both unfilled and filled compounds.
7. Enclosed gas pressure in the closed cell increases the relative modulus value in 30 phr carbon black filled compounds, whereas relative tensile strength decreases sharply and does not follow the additive rule.
8. The stress-relaxation bahavior is independent of the blowing agent loading, i.e., density of closed-cell microcellular rubber.
9. The hysteresis loss decreases with the increase in blowing agent concentration due to the elastic behavior of the closed cell.
10. Theoretically calculated flaw sizes in tensile rupture are found to be about 3.4 times larger than the maximum cell size measured from SEM photomicrographs of razor-cut closed-cell microcellular rubber samples. It suggests that tear path deviates from the linear front and gives rise to a larger effective depth of the flaws.

We are grateful to the Council of Scientific and Industrial Research, Government of India, for financial support for this work.

REFERENCES

1. S. K. Bose, *Rubb. World,* **108**(5), 23 (1993).
2. D. G. Rowland, *Rubb. World,* **108**(5), 27 (1993).
3. D. G. Rowland, *Rubb. Chem. Technol.,* **66**(3), 463 (1993).
4. W. R. Randall and J. A. Reidel, *Rubb. World,* **207**(4), 23 (1993).
5. M. A. Albam and A. P. Pisarenko, *Sov. Rubb. Technol.,* **18,** 22 (1959).
6. L. Spenadel, *Rubb. World,* **150**(5), 69 (1964).
7. R. C. Bascom, *Rubb. Age,* **95**(4), 576 (1964).
8. D. R. Filburn and L. Spenadel, *Rubb. Age,* **102**(11), 37 (1970).
9. C. S. Wang, *J. Appl. Polym. Sci.,* **27,** 1205 (1982).
10. J. H. Aubert, *J. Cell. Plast.,* **24**(3), 132 (1988).
11. L. J. Gibson and M. F. Ashby, *Cellular Solids, Structure and Properties,* Pergamon Press, Oxford, 1988.
12. R. W. Pekala, C. T. Alviso, and J. D. Lemay, *J. Non-Cryst. Solids,* **125,** 67 (1990).
13. L. J. Gibson, *Mater. Sci. Eng. A,* **110,** 1 (1989).
14. A. N. Gent and A. G. Thomas, *J. Appl. Polym. Sci.,* **2**(6), 354 (1959).
15. A. N. Gent and A. G. Thomas, *J. Appl. Polym. Sci.,* **1**(1), 107 (1959).
16. A. N. Gent and A. G. Thomas, *Rubb. Chem. Technol.,* **36,** 597 (1963).
17. J. M. Lederman, *J. Appl. Polym. Sci.,* **15,** 693 (1971).
18. C. W. Stewart, *J. Polym. Sci. A2,* **8** (1970).
19. J. H. Exelby, *Plast. Rubb. Comp. Proc. Appl.,* **15**(4), 213 (1991).
20. A. Dutta and M. Cakmak, *Rubb. Chem. Technol.,* **65**(5), 778 (1992).
21. N. S. Ramesh, D. H. Rasmussen, and G. A. Cambell, *Polym. Eng. Sci.,* **31**(23), 1657 (1991).

22. J. S. Cotton and N. P. Suh, *Polym. Eng. Sci.*, **27**(7), 493 (1987).
23. V. Kumar and N. P. Suh, *Polym. Eng. Sci.*, **30**(20), 1323 (1990).
24. K. Mukhopadhyay, D. K. Tripathy, and S. K. De, *Rubb. Chem. Technol.*, **66**(1), 38 (1993).
25. R. E. Whitteker, *J. Appl. Polym. Sci.*, **15,** 1205 (1971).
26. C. Hepburn and N. Alam, *Cell Polym.*, **10**(2), 99 (1991).
27. P. D. Agarwal and K. E. Kear, *Rubb. World,* **201**(6), 20 (1990).
28. K. C. Guriya and D. K. Tripathy, *Plast. Rubb. Comp. Proc. Appl.*, **23**(3), 195 (1995).
29. R. S. Rivlin and A. G. Thomas, *J. Polym. Sci.*, **10,** 291 (1953).

Received January 11, 1996
Accepted April 16, 1996